

Measured Uplink Interference Caused by Aerial Vehicles in LTE Cellular Networks

Raphael Amorim¹, Huan Nguyen¹, Jeroen Wigard, István Z. Kovács, Troels B. Sørensen, David Z. Biro, Mads Sørensen, and Preben Mogensen

Abstract—Aerial users, such as unmanned aerial vehicles (UAVs), experience different radio propagation conditions than users on the ground. This is a concern regarding the integration of such users into cellular networks in the near future. This letter investigates the impact of uplink transmissions from an aerial user equipment. Full buffer transmissions were performed by a device at ground level and also flying attached to a UAV at 100 m height. The field measurements show a higher number of cells affected by the aerial transmission, with an increase of up to 7.7 dB in the interference over thermal noise in cells within 15 km of the test location. This letter also assesses two strategies to reduce the uplink interference caused by aerial users: 1) UAV's cruise height control and 2) directional transmissions. Results show the directional transmission is a more promising technique, and has the advantage of not reducing the uplink received power.

Index Terms—UAVs, air to ground channel, aerial communication.

I. INTRODUCTION

UNMANNED Aerial Vehicle (UAVs), also known as drones, are experiencing a market surge boosted by technological developments in recent years. Data connectivity is one of the key enablers for beyond visual line-of-sight (BVLOS) flight ranges, which can help to unleash an emerging potential. Besides the control link between UAVs and their users, many applications may require high data rate connectivity, such as surveillance, infrastructure monitoring, and

media streaming [1]. Cellular networks are ubiquitous, have a ready-to-market implemented infrastructure and are capable of supporting broadband applications. Therefore, they arise as natural candidates to provide UAVs's connectivity.

The Third Generation Partnership Project (3GPP) has opened a work item on enhanced support for aerial vehicles [2] to set common ground for performance evaluation of such devices. At the time of writing, current channel models are assumed to be height dependent and approximate free space propagation as UAV moves up. Galkin *et al.* [3] use stochastic geometry to show that the aerial devices present higher line-of-sight (LOS) probability than users on the ground. Preliminary results in [4] and [5] indicate this may change the interference patterns commonly observed in cellular networks.

Understanding how less severe path losses impact the performance of both new aerial and legacy users is a topic of interest for network operators [6]. This letter is focused on the performance assessment of uplink (UL) transmissions, i.e., from the user equipment (UE), either ground or aerial, to the base station (BS). Previous studies in [7] and [8] use downlink (DL) field measurements to estimate the UL interference power observed by the neighbor cells detected in the experiment. Results indicate a significant increase in the UL interference power as a function of the UE height.

In this letter, UL field measurements were performed in a rural area in Denmark, using a commercial Long-Term Evolution (LTE) carrier at 800 MHz. A test phone performed transmissions at two different heights: on ground level and attached to an airborne UAV at 100 m, a height compatible with many UAV's commercial applications. A collaboration with the network operator enabled the assessment of the impact of such transmissions in all the co-channel cells within a 15 km radius area. Based on the observations, this letter discusses the challenges of implementing interference coordination techniques and presents two other possible countermeasures to the high interference. The first, UAV cruise height control, is based on observations made in [9] and [10] that UAVs' height may be optimized, offering a trade off between throughput and interference in adjacent cells. The second strategy, directional array of antennas at the UAV, tries to minimize the interference without sacrificing the user throughput based on evidences presented in [11].

The remainder of this letter is organized as follows: Section II addresses the setup and details of the field measurements; Section III shows the measured results and discuss their implications. Final remarks are found in Section IV.

Manuscript received February 5, 2018; revised May 8, 2018; accepted May 17, 2018. Date of publication May 30, 2018; date of current version December 14, 2018. This work was supported by SESAR Joint Undertaking through the European Union's Horizon 2020 Research and Innovation Programme under Grant 763601. The associate editor coordinating the review of this paper and approving it for publication was P. A. Dmochowski. (Corresponding author: Raphael Amorim.)

R. Amorim, H. Nguyen and T. B. Sørensen are with the Wireless Communications Networks Section, Department of Electronic Systems, Aalborg University, 9220 Aalborg, Denmark (e-mail: rma@es.aau.dk; hcn@es.aau.dk; e-mail: tbs@es.aau.dk).

J. Wigard and I. Z. Kovács are with Nokia Bell Labs Aalborg, 9220 Aalborg, Denmark (e-mail: jeroen.wigard@nokia-bell-labs.com; istvan.kovacs@nokia-bell-labs.com).

D. Z. Biro is with the Department of Technology, Service Development, Analytic Platforms, Telenor, 9000 Aalborg, Denmark (e-mail: dazb@telenor.dk).

M. Sørensen is with the Department of Network Services, Telenor, 9000 Aalborg, Denmark (e-mail: mds@telenor.dk).

P. Mogensen is with the Wireless Communications Networks Section, Department of Electronic Systems, Aalborg University, 9220 Aalborg, Denmark, and also with Nokia Bell Labs Aalborg, 9220 Aalborg, Denmark (e-mail: pm@es.aau.dk).

Digital Object Identifier 10.1109/LWC.2018.2841386

TABLE I
MONITORED CELLS INFORMATION

	Average	Minimum	Maximum
Height (meters)	37.2	27.5	54
Downtilt (degrees)	5.2	3	8

II. FIELD MEASUREMENTS SETUP

A. Network Scenario

The monitored area includes 50 live operating cells distributed over 17 sites. Reference information for the base stations, such as average, maximum and minimum values for antennas downtilt and transmitter heights, is found in Table I. In order to minimize the impact to and from other users in the network, the measurements were performed at night, between 2-5 AM. In this time window, the average UL cell measured in the two weeks previous to the test was only 2 percent.

B. Test Device and Operation

The tests were carried out with an R&S QualiPoc¹ Android smartphone. In order to obtain a full-buffer behavior, a large test file (approximately 400 MB) was repeatedly transmitted by the device, that was locked to a 10 MHz LTE carrier in the 800 MHz band. The tests, which had 15 minutes of duration, were repeated three times for each of the two cases: the terrestrial UE (TUE), from a static ground position at 1.5 m, and the airborne UE (AUE) at 100 m, with the smartphone attached to a UAV flying in circles of 7 m radius.

C. Measurements

For this analysis the interference over thermal noise power (IoT) in the network cells was provided by the telecom operator. This performance indicator reports the median of the noise rise in LTE Physical Uplink Shared Channel (PUSCH) [12] sub-bands over periods of 15 minutes. For each test, starting and ending time were synchronized with the report generated at the base stations.

Reports were also collected by the phone software. UL measurements include phone's average transmit power, number of Physical Resource Blocks (PRBs) used and throughput in PUSCH channel. DL measurements include physical cell indicator (PCI) and reference signal received power (RSRP) [12] for the serving cell and for some detected neighbors. During the trials, sampling rates observed were around 0.8-2 Hz.

III. RESULTS AND DISCUSSION

Before comparing the impact on UL in the two cases, it is important to understand how these transmissions compare to each other, especially regarding the transmit power. Figure 1 shows the CDF of three metrics recorded by the phone across all tests: UL transmit (Tx) Power, PRBs used in PUSCH Channel and PUSCH throughput. Despite UL power control in LTE base stations, UE is transmitting close to its maximum power, 23 dBm, in both cases, indicating a power-limited

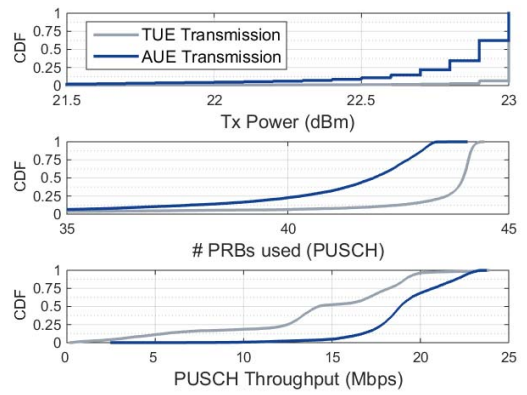


Fig. 1. Cumulative Density Function (CDF): Recorded Tx Power, PRB usage and UL throughput for the transmissions using the terrestrial user equipment (TUE) and the airborne user equipment (AUE).

throughput due to the path loss. A slightly lower average output power, 22.8 dBm, is observed by the AUE, compared to the TUE (23.0 dBm). In addition, TUE and AUE also show similar average resource usage, occupying 42.8 and 40.8 PRBs respectively, which indicates similar power spectral density in both cases. Also, the bandwidth used was close to the maximum number of PRBs available for PUSCH in a 10 MHz bandwidth (46), corroborating the assumption of low network load generated by other users.

Despite these similarities, the median throughput obtained during aerial transmissions is 32.5 percent higher than that observed at ground level (18.9 versus 14.2 Mbps). This can be attributed to lower coupling losses, as indicated by the phone reports. The AUE case reported higher average Modulation and Coding Scheme (MCS) than the TUE case, 23.7 versus 18.7, and higher median serving cell DL Reference Signal Received Power (RSRP), -94 dBm versus -101 dBm. It is worth noting that the TUE and the UAV are not connected to the same serving cell. The TUE's serving cell is 3.8 km away, but the AUE made a handover to a farther serving cell (13.7 km away) after taking off, probably because its new elevated position was in a low gain region of the closest cell's antenna.

The IoT was evaluated to quantify the impact of such transmissions to the cells in the vicinity. The average IoT for each base station across the three tests was used as a metric for comparison. The previous two weeks of measurements, within the same time frame (2-5 AM), was used as a baseline value for each cell. If the IoT for either AUE or TUE exceeds the 99th percentile of the baseline, the cell is considered an Interference Victim Cell (IVC). This is motivated on the ground that it is more likely that the transmissions of the test device caused the outlier, rather than statistical variation.

A total of 20 cells were classified as IVCs. Fig. 2 shows all IVCs ranked by the higher IoT in the AUE test. The same figure shows the boxplots for the IoT distribution in the baseline data for each IVC. The IoT reference line at 1.6 dB marks the highest IoT baseline value observed. It is possible to see that the IoT caused by the AUE is much higher than that caused by a similar transmission at ground level. For instance, only in 6 cells the IoT caused by the TUE is above the 1.6 dB

¹More information about the QualiPoc software in https://www.rohdeschwarz.com/us/brochure-datasheet/qualipoc_android/.

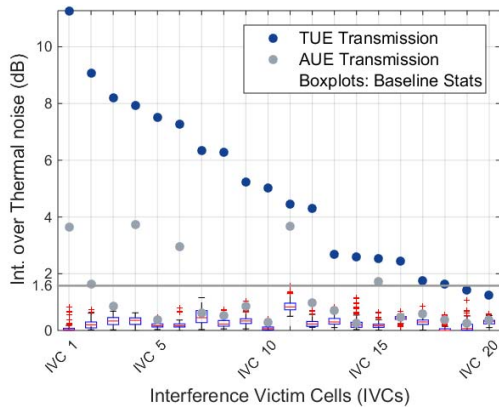


Fig. 2. Interference over Thermal Noise (IoT) per Interference Victim Cells (IVCs). IVCs indexes are ranked by higher IoT values.

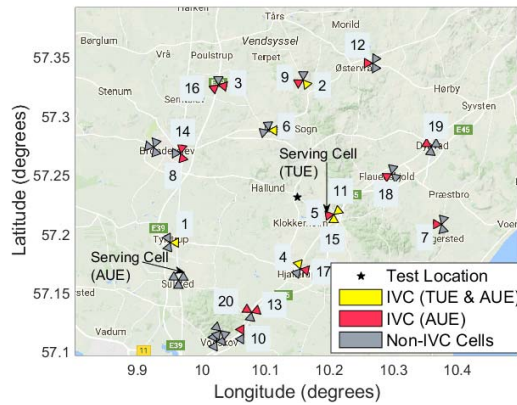


Fig. 3. IVC cells map distribution. Numbers identify the IVC index.

reference line, while 18 cells exceed this threshold for the AUE transmission. The average IoT increase is 3.7 dB, with peaks between 7.1 and 7.7 dB (IVCs 1, 2, 3 and 5), in spite of the downtilted antennas, which should partially reject the transmission received from the UAV.

Fig. 3 shows the spatial distribution of the IVCs on the map. IVCs 7, 18 and 19 are located behind a hill from the test location perspective, and interference prediction tools would not account for harmful signal levels originated by the test location. This effect will be especially important for interference prediction in urban areas, where buildings are accounted for significant interference containment.

Predefining the set of neighbor cells for interference coordination will be difficult as results indicate the set of impacted cells varies with height. Moreover, optimizing a coordinated scheduling for AUE over such a large set of impacted cells would lead to significant reduction in overall resource availability in the network. Besides, it may be too complex to be performed in real time, especially when several UAVs are using broadband services at the same time. This letter analyses two strategies to mitigate the interference caused by an AUE without dealing with resource coordination: 1) cruise height control and 2) directional antennas transmission.

The radio reports collected by the UE may provide valuable information to estimate the IoT reduction that can be

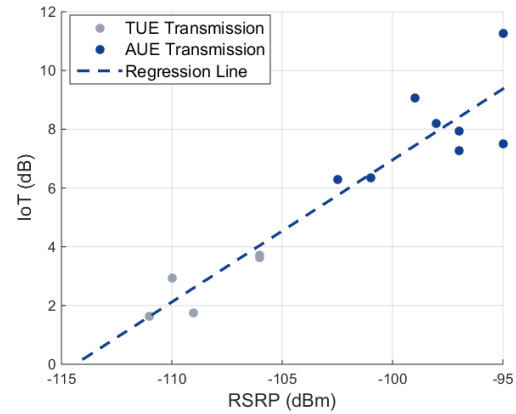


Fig. 4. IoT versus downlink reference symbol received power (RSRP) from neighbor cells.

achieved by both techniques. The DL RSRP seems to provide good estimation for the coupling losses between UE and surrounding cells, despite the frequency duplexing [8]. Fig. 4 shows how DL RSRP measurements correlate to IoT values, for the cells the phone was able to detect. It is possible to see that the regression line performs a good estimation for the potential UL interference power. It is important to note that cells outside the monitored area were also detected by AUE with high RSRP. The most significant case was observed at a cell located approximately 30 km from the test location, whose median RSRP of -97 dBm estimates an IoT of about 8 dB.

Results in [4] and [6] indicate a negative effect of increasing UAV height in DL interference. Assuming the network and the AUE can negotiate the cruise height, constrained to UAV's application requirements, it is possible to reduce the interference power in both UL and DL. In this letter it is estimated the UL IoT reduction obtained by decreasing AUE's height to 50 and 25 m. For this calculation, it is first estimated the path loss difference between 100 m (test height) and the two target heights (50 m and 25 m) using the channel model proposed in [5]. Then, the IoT reduction correspondent to such decrease in received power is estimated by applying the linear relation given by the slope of the line in Fig. 4. No changes in BSs's antenna gains are considered, as changes in the elevation angle are assumed negligible due to the distances between most IVCs and the test location (>10 km) [13]. If this calculation results in a very low estimated IoT for a given cell, the baseline median for that cell is used as a lower boundary to account for residual IoT in the network.

Results are shown in Fig. 5, where it is possible to see that lower AUE heights lead to smaller IoT at the IVCs. At 50 m, the estimated IoT is on average 2.1 dB higher than the values measured for the TUE. This value decreases to 0.9 dB at 25 m. Nevertheless, this solution reduces the serving cell RSRP that would drop from -94 dBm, at 100 m, to -99 dBm (50 m) and -104 dBm (25 m), which indicates a trade-off between interference and AUE throughput.

The other solution relies on the fact most commercial UAVs are not restricted to small form factor and therefore they may

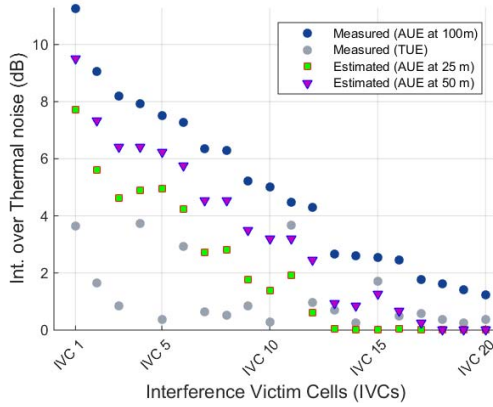


Fig. 5. IoT measured in the tests compared to estimated values obtained for AUE at 25 and 50 m. The estimations consider the differences in path loss for different heights in the channel model proposed in [5].

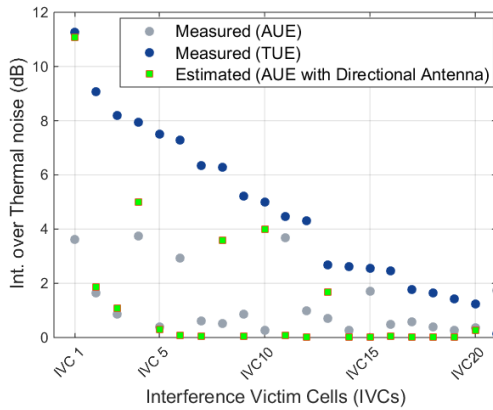


Fig. 6. Measured IoT versus the estimated IoT from introducing a directional antenna model on the AUE.

deploy an array of antennas with directional pattern to mitigate the UL and DL interference with the advantage of causing minor impact on the serving cell signal. To evaluate this potential, it was estimated the IoT reduction obtained by applying the directional antenna pattern suggested in [2] and shown in eq. (1) (in dB). In this equation, the main direction, $\theta = 0^\circ$, is the direction of maximum antenna gain, G_{max} , set to 0 dB, and θ_{3dB} is the half-power beam width.

$$G(\theta) = G_{max} - \min \left[12 \left(\frac{\theta}{\theta_{3dB}} \right)^2, 20 \right] \quad (1)$$

Results were estimated considering a wide-beam case where $\theta_{3dB} = 70^\circ$ and a perfect alignment, that means the UAV antenna main direction point towards the serving cell. Results in Fig. 6 show significant IoT reduction obtained with the use of directional antennas in the AUE. The IoT values are similar to that observed by the TUE transmission, with an average difference of 0.3 dB. Additionally, as the effective transmit power in the main direction is the same as the reference case, the throughput towards the serving cell will remain unchanged. However, the directional beam cannot prevent high interference levels at cells located close to the serving cell, for example IVC 1 (see Fig. 3). Furthermore, estimations show the

applied wide beam is robust to misalignment up to $\pm 15^\circ$ from the maximum power direction.

IV. CONCLUSION

This letter presents one of the challenges of having UAVs connected to the LTE cellular networks. Measurements were conducted by having a test phone transmitting full-buffer data at two heights, 1.5 m and 100 m. Results show similar UL transmit power and allocated resources, but the UAV at 100 m tends to cause significantly more interference than the UE at 1.5 m. The UAV causes an interference over thermal noise (IoT) 3.7 dB higher on average than that caused by the terrestrial UE, with peaks at between 7 and 8 dB. High interference is measured in cells up to 14 km away, but results indicate this distance may be as high as 30 km. Both the UAV cruise height control and the use of directional antennas at the UAV side showed potential to reduce the interference caused by UAVs to values comparable to those observed due to a terrestrial UE. The latter seems to be more promising as it can be achieved without reducing the user throughput.

ACKNOWLEDGMENT

The research is conducted as part of the DroC2om project. The authors would also like to acknowledge the contribution of Steffen Hansen and Daniel Kappers to the UAV flights.

REFERENCES

- [1] "Evolving cellular technologies for safer drone operation," San Diego, CA, USA, Qualcomm Technol. Inc., White Paper, Oct. 2016.
- [2] *Enhanced LTE Support for Aerial Vehicles 3rd Generation Partnership Project (3GPP) Version 15.0.0*, 3GPP Standard TS 36.777, Jan. 2018.
- [3] B. Galkin, J. Kibilda, and L. A. D. Silva, "Coverage analysis for low-altitude UAV networks in urban environments," in *Proc. IEEE Glob. Commun. Conf.*, Singapore, Dec. 2017, pp. 1–6.
- [4] B. V. D. Bergh, A. Chiumento, and S. Pollin, "LTE in the sky: Trading off propagation benefits with interference costs for aerial nodes," *IEEE Commun. Mag.*, vol. 54, no. 5, pp. 44–50, May 2016.
- [5] R. Amorim *et al.*, "Radio channel modeling for UAV communication over cellular networks," *IEEE Wireless Commun. Lett.*, vol. 6, no. 4, pp. 514–517, Aug. 2017.
- [6] M. M. Azari, F. Rosas, A. Chiumento, and S. Pollin, "Coexistence of terrestrial and aerial users in cellular networks," in *Proc. IEEE Glob. Commun. Conf. Workshops*, Singapore, Dec. 2017, pp. 1–6.
- [7] I. Kovacs, R. Amorim, H. C. Nguyen, J. Wigard, and P. Mogensen, "Interference analysis for UAV connectivity over LTE using aerial radio measurements," in *Proc. IEEE 86th Veh. Tech. Conf. (VTC Fall)*, Toronto, ON, Canada, Sep. 2017, pp. 1–6.
- [8] *LTE Unmanned Aircraft Systems Trial Report*, San Diego, CA, USA, Qualcomm Technol. Inc., White Paper, May 2017.
- [9] M. Mozaffari, W. Saad, M. Bennis, and M. Debbah, "Unmanned aerial vehicle with underlaid device-to-device communications: Performance and tradeoffs," *IEEE Trans. Wireless Commun.*, vol. 15, no. 6, pp. 3949–3963, Jun. 2016.
- [10] A. Al-Hourani, S. Kandeepan, and A. Jamalipour, "Modeling air-to-ground path loss for low altitude platforms in urban environments," in *Proc. IEEE Glob. Commun. Conf.*, Austin, TX, USA, Dec. 2014, pp. 2898–2904.
- [11] H. C. Nguyen *et al.*, "How to ensure reliable connectivity for aerial vehicles over cellular networks," *IEEE Access*, vol. 6, pp. 12304–12317, 2018.
- [12] *Evolved Universal Terrestrial Radio Access (E-UTRA); Physical Channels and Modulation 3rd Generation Partnership Project (3GPP) Version 8.9.0*, 3GPP TS Standard 36.211, Dec. 2009.
- [13] A. Al-Hourani and K. Gomez, "Modeling cellular-to-UAV path-loss for suburban environments," *IEEE Wireless Commun. Lett.*, vol. 7, no. 1, pp. 82–85, Feb. 2018.